Original Article | Neuroimaging and Head & Neck

eISSN 2005-8330
https://doi.org/10.3348/kjr.2020.1272
Korean J Radiol 2021;22(8):1369-1378

Korean Journal of Radiology
KJR

Prognostic Prediction Based on Dynamic Contrast-Enhanced MRI and Dynamic Susceptibility Contrast-Enhanced MRI Parameters from Non-Enhancing, T2-High-Signal-Intensity Lesions in Patients with Glioblastoma

Sang Won Jo[1], Seung Hong Choi[2, 3], Eun Jung Lee[4], Roh-Eul Yoo[2], Koung Mi Kang[2], Tae Jin Yun[2], Ji-Hoon Kim[2], Chul-Ho Sohn[2]

[1]Department of Radiology, Hallym University Dongtan Sacred Heart Hospital, Hwaseong, Korea; [2]Department of Radiology, Seoul National University Hospital, Seoul, Korea; [3]Center for Nanoparticle Research, Institute for Basic Science, and School of Chemical and Biological Engineering, Seoul National University, Seoul, Korea; [4]Department of Radiology, Human Medical Imaging & Intervention Center, Seoul, Korea

Objective: Few attempts have been made to investigate the prognostic value of dynamic contrast-enhanced (DCE) MRI or dynamic susceptibility contrast (DSC) MRI of non-enhancing, T2-high-signal-intensity (T2-HSI) lesions of glioblastoma multiforme (GBM) in newly diagnosed patients. This study aimed to investigate the prognostic values of DCE MRI and DSC MRI parameters from non-enhancing, T2-HSI lesions of GBM.

Materials and Methods: A total of 76 patients with GBM who underwent preoperative DCE MRI and DSC MRI and standard treatment were retrospectively included. Six months after surgery, the patients were categorized into early progression (n = 15) and non-early progression (n = 61) groups. We extracted and analyzed the permeability and perfusion parameters of both modalities for the non-enhancing, T2-HSI lesions of the tumors. The optimal percentiles of the respective parameters obtained from cumulative histograms were determined using receiver operating characteristic (ROC) curve and univariable Cox regression analyses. The results were compared using multivariable Cox proportional hazards regression analysis of progression-free survival.

Results: The 95th percentile value (PV) of Ktrans, mean Ktrans, and median Ve were significant predictors of early progression as identified by the ROC curve analysis (area under the ROC curve [AUC] = 0.704, p = 0.005; AUC = 0.684, p = 0.021; and AUC = 0.670, p = 0.0325, respectively). Univariable Cox regression analysis of the above three parametric values showed that the 95th PV of Ktrans and the mean Ktrans were significant predictors of early progression (hazard ratio [HR] = 1.06, p = 0.009; HR = 1.25, p = 0.017, respectively). Multivariable Cox regression analysis, which also incorporated clinical parameters, revealed that the 95th PV of Ktrans was the sole significant independent predictor of early progression (HR = 1.062, p < 0.009).

Conclusion: The 95th PV of Ktrans from the non-enhancing, T2-HSI lesions of GBM is a potential prognostic marker for disease progression.

Keywords: *Glioblastoma multiforme; Dynamic contrast-enhanced MR imaging; Dynamic susceptibility contrast MR imaging; Prognosis prediction; Peritumoral area*

Received: October 22, 2020 **Revised:** December 15, 2020 **Accepted:** January 8, 2021

This study was funded by a grant from the Korea Healthcare technology R&D Projects, Ministry for Health, Welfare & Family Affairs (HI16C1111), by the Brain Research Program through the National Research Foundation of Korea (NRF) funded by the Ministry of Science, ICT & Future Planning (2016M3C7A1914002), by Basic Science Research Program through the National Research Foundation of Korea (NRF) funded by the Ministry of Science, ICT & Future Planning (2020R1A2C2008949), by Basic Science Research Program through the National Research Foundation of Korea (NRF) funded by the Ministry of Science, ICT & Future Planning (NRF-2019K1A3A1A77079379), by Creative-Pioneering Researchers Program through Seoul National University (SNU), and by the Institute for Basic Science (IBS-R006-A1).

Corresponding author: Seung Hong Choi, MD, PhD, Department of Radiology, Seoul National University Hospital, 101 Daehak-ro, Jongno-gu, Seoul 03080, Korea.
• E-mail: verocay@snuh.org

INTRODUCTION

Glioblastoma multiforme (GBM) is the most common and aggressive primary brain tumor. It is a highly malignant tumor with a median survival of 14 months following standard treatment, including surgical resection and radiochemotherapy [1]. Generally, GBM is a hypervascular tumor, and its contrast-enhancing portion is the main target of standard treatment regimens because it is the most aggressive. T2-weighted or T2 fluid-attenuated inverse recovery (FLAIR) images reveal non-enhancing, T2-high-signal-intensity (T2-HSI) lesions surrounding the GBM (excluding the contrast-enhancing portion and cystic or necrotic components). These lesions usually persist after the surgical removal of the contrast-enhancing area of GBM, which is the first step of standard GBM treatment [2,3]. Recurrence typically develops around the primary tumor site [4-6], which may be attributed to the residual non-enhancing, infiltrated tumor cells. Non-enhancing, T2-HSI lesions consist of a mixture of reactive edema and infiltrative tumor tissue [1,7,8], which are difficult to differentiate using only morphological images. Therefore, it is important to identify the techniques for investigating residual infiltrative tumor tissue noninvasively. Because an immature microvascular structure and microvascular leakage are associated with active angiogenesis in GBM, tumor microvessel leakiness can be used as a noninvasive prognostic predictor for patients with this type of tumor. Perfusion- and permeability-based imaging modalities provide functional imaging information about the capillary ultrastructure and physiological microvascular properties of non-enhancing, T2-HSI lesions and could provide additional prognostic information for GBM.

A few previous studies have focused on the perfusion or permeability parameters of non-enhancing, T2-HSI lesions for identifying key prognostic features [9-11]. To the best of our knowledge, no previous studies have evaluated dynamic contrast-enhanced (DCE) MRI and dynamic susceptibility contrast (DSC) MRI together for the prediction of early progression (EP) using non-enhancing, T2-HSI lesions in GBM patients. Therefore, our retrospective study evaluated DSC MRI and DCE MRI parameters from non-enhancing, T2-HSI lesions of GBM for predicting EP (PFS of ≤ 6-months after surgery) in the patients who underwent total tumor resection of the contrast-enhancing portion followed by radiotherapy plus concomitant maintenance treatment with temozolomide.

MATERIALS AND METHODS

Patients

Our Institutional Review Board approved this single-center retrospective study, and the requirement for written informed consent was waived (IRB No. H-2008-031-1145). From April 2010 through May 2017, a total of 269 patients with newly confirmed GBM at our hospital were consecutively enrolled in this study. The patients were included if they were 1) adults (older than 18 years of age) with histopathological confirmation of GBM based on the World Health Organization 2016 classification of CNS tumors, 2) underwent both preoperative DCE MRI and DSC MRI, and 3) had received standard treatment, including total resection of contrast-enhancing portions of the tumor, ensuing concurrent chemoradiation therapy (CCRT), and adjuvant temozolomide treatment. Eventually, 76 patients with GBM were included in this study.

All the patients underwent follow-up brain MRI every 3 months for the first 2 years when they visited the outpatient clinic. Thereafter, the follow-up interval was prolonged to half a year in the absence of clear clinical or radiologic evidence of tumor progression. At each time point, the assessment of the treatment response and categorization of the patients into EP and non-EP (NEP) groups was performed and double-checked by clinicians and radiologists based on the Response Assessment in Neuro-Oncology (RANO) criteria [12]. Consequently, at the 6-month follow-up, 15 patients (20%, 15/76) were allocated to the EP group, and 61 patients (80%, 61/76)

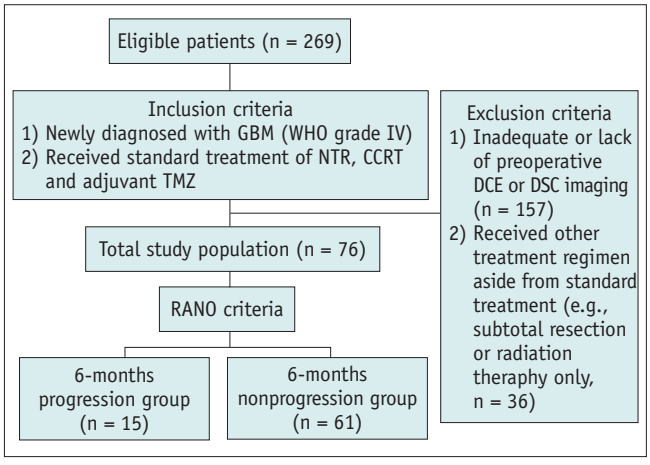

Fig. 1. Study design flow chart. CCRT = concomitant chemoradiotherapy, DCE = dynamic contrast-enhanced, DSC = dynamic susceptibility contrast, GBM = glioblastoma multiforme, NTR = near-total resection of contrast-enhancing portion, RANO = response assessment in neuro-oncology, TMZ = temozolomide

https://doi.org/10.3348/kjr.2020.1272

Korean Journal of Radiology
KJR

were allocated to the NEP group. The flow diagram in Figure 1 illustrates the inclusion and exclusion of patients in this study.

Image Acquisition

Imaging acquisition techniques and the specific MRI parameters for all the sequences are depicted in Supplementary Materials 1 and Supplementary Table 1.

Postprocessing and Image Analysis of DCE MR Imaging and DSC MR Imaging

Detailed postprocessing steps for the DCE and DSC MR images are summarized in Supplementary Materials 2, and the image analysis is described in Supplementary Materials 3 and illustrated in Supplementary Figure 1.

Statistical Analysis

The data for each parameter were evaluated for normality using the Kolmogorov-Smirnov test.

The student's *t* test was performed for normally distributed data, and the Mann-Whitney U test was performed for non-normally distributed data. Fisher's exact test or the chi-squared test was used to compare categorical variables among the clinical characteristics of the EP and NEP groups.

The means or medians of the permeability and perfusion parameter values of the two groups were compared using the Student's *t* test or the Mann-Whitney U test.

Spearman's rank correlation analysis and the calculation of intraclass correlation coefficients were performed to reveal the correlations between the normalized relative cerebral blood volume (nCBV) from the DSC MRI and the permeability parameters from the DCE MRI.

We determined the cumulative histograms for the permeability and perfusion parameters (Ktrans, Ve, Vp and nCBV) (the Xth percentile point is the point at which X% of the voxel values that form the histogram are found to the left of the histogram) based on the findings of the previous studies [13,14]. Afterward, we found the optimal percentile point with the highest area under the receiver operating characteristic (ROC) curve for distinguishing between the EP and NEP groups. The significance (*p* value) of the areas under the receiver operating curves (AUCs) were test by comparing with a random guess (AUC = 0.50). After the ROC curve analysis, survival was analyzed using univariable Cox regression.

If any of the quantitative permeability and perfusion parameters of DCE or DSC MRI reached statistical significance during the aforementioned statistical analysis, they were included in the multivariable Cox proportional hazard regression to analyze its correlation with prognosis.

The Kaplan-Meier survival analysis was used to predict early disease progression using statistically significant parameters. The survival curves were compared using the log-rank test.

The statistical analyses were performed using two statistical software programs (SPSS, Version 21.0 for

Table 1. Baseline Characteristics of the Study Population*

Parameter	Total (n = 76)	EP (n = 15)	NEP (n = 61)	*P*
Mean age, years	56.6 (22–77)	57.2	56.4	0.83†
Radiation dose, Gy	56.8 ± 8.2	56.1 ± 12.2	57.0 ± 7.0	0.70†
Sex				0.51‡
Male	45	10	35	
Female	31	5	26	
Genetic information				
IDH mutation				1.00§
Mutant	2	0	2	
Wild-type	74	15	59	
MGMT promoter				0.69‡
Methylated	37	8	29	
Unmethylated	39	7	32	
Karnofsky performance score				0.44§
< 70	12	1	11	
70	64	14	50	

Data represent the number of patients, unless otherwise noted. *Data are mean ± standard deviation, †Calculated with student's *t* test, ‡Calculated with the chi-square test, §Calculated with Fisher's exact test. EP = early progression, IDH =isocitrate dehydrogenase, MGMT = O6-methylguanine-DNA methyltransferase, NEP = nonearly progression

https://doi.org/10.3348/kjr.2020.1272

Windows, IBM Corp.; MedCalc, Version 18.11 for Windows, MedCalc Software). For all the statistical analyses, the results were accepted as statistically significant only if the probability value was less than 0.05.

RESULTS

Baseline Patient Clinical Characteristics

The mean age of the overall study population was 56.6 ± 2.9 years, and 45 male and 31 female patients were included in the study. The median PFS of our study population was 10.1 months (302.5 days).

None of the characteristics of the patients, such as age, sex, radiation dose, Karnofsky performance status score, isocitrate dehydrogenase mutation status, and O6-methylguanine-DNA methyltransferase (MGMT) promoter methylation status, significantly differed between the EP and NEP groups (all $p > 0.05$). The clinical and genetic characteristics of the patients in the EP and NEP groups are summarized in Table 1.

Table 2. Permeability Parameters with Significant Differences between the EP and NEP Groups

Permeability Parameter	PFS Group	Median	IQR	*P**
Ktrans 95th PV	NEP	0.0258	0.0325	0.015
	EP	0.0484	0.0414	
Mean Ktrans	NEP	0.0120	0.0117	0.026
	EP	0.0165	0.0350	
Median Ve	NEP	1.30	1.35	0.042
	EP	2.00	2.50	

*Calculated with the Mann-Whitney U test. EP = early progression, IQR = interquartile ranges, NEP = nonearly progression, PFS = progression-free survival, PV = percentile value

Differences in Permeability and Perfusion Parameters between EP and NEP Groups

For DCE and DSC MRI, the nCBV showed a normal distribution, but Ktrans, Ve, and Vp did not. The mean Ktrans and median Ve were significantly higher in the EP group than in the NEP group ($p = 0.026$ and $p = 0.042$, respectively). In contrast, the mean or median values of Vp and nCBV did not significantly differ in the groups ($p > 0.05$; Supplementary Table 2). Table 2 and Figure 2 show the specific values and ranges of the mean Ktrans and median Ve of the two groups.

The results of the correlation analysis of the permeability parameters from DCE MRI and nCBV from DSC MRI are shown in Supplementary Table 3, Supplementary Figure 2, and Supplementary Results.

Cumulative Histogram Analysis and ROC Curve Analysis of Permeability and Perfusion Parameters to Differentiate the EP and NEP Groups

After analyzing the cumulative histogram of Ktrans, the 95th percentile value (PV) of Ktrans (range: 90–100th PV Ktrans) demonstrated the highest area under the curve (AUC) for EP prediction with a value of 0.704 ($p = 0.005$). In contrast, there were no statistically significant PVs for predicting EP in the cumulative histograms of Ve, Vp, or nCBV ($p > 0.05$).

ROC curve analysis was also performed to assess the prognostic performance of the DCE MRI permeability

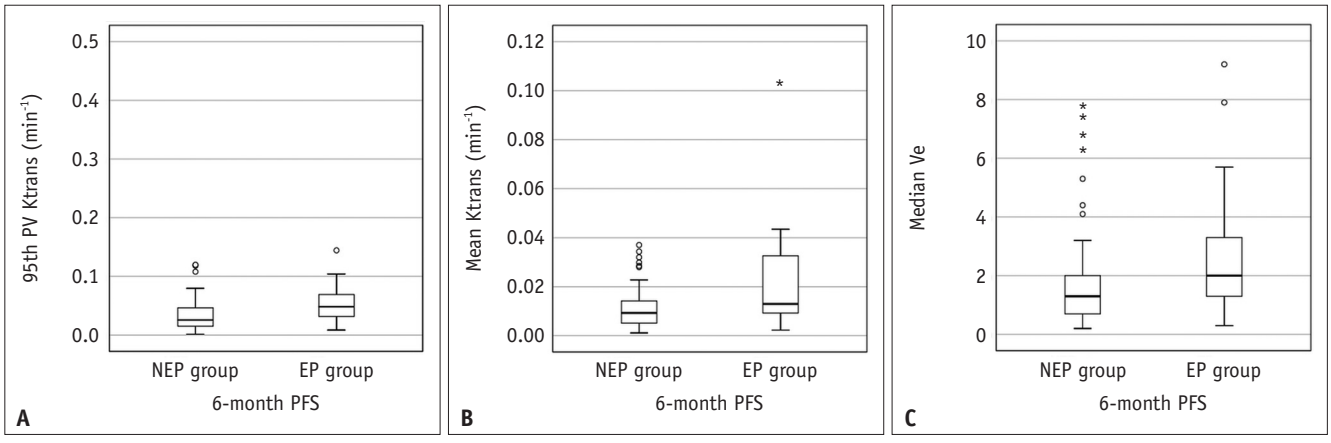

Fig. 2. Box-whisker plots showing significant differences between the permeability parameters (95th PV of Ktrans, Mean Ktrans, and Median Ve) (A, B, and C, respectively) of the NEP and EP groups. The lines inside the boxes and the lower and upper box boundary lines represent the median and the 25th and 75th PVs, respectively, with whiskers extending from the median to ± 1.5 x interquartile ranges and outliers beyond the whiskers represented by points. EP = early progression, NEP = non-EP, PFS = progression-free survival, PV = percentile value

https://doi.org/10.3348/kjr.2020.1272

Korean Journal of Radiology
KJR

Table 3. ROC Curve Analysis of the Statistically Significant Permeability Parameters for Differentiating the Early Progression and Nonearly Progression Groups

Permeability Parameter	AUC	Cutoff	*P**	Sensitivity	Specificity	*P*†
95th PV Ktrans	0.704	0.0312	0.005	80.0	57.4	> 0.05
Mean Ktrans	0.684	0.0122	0.021	73.3	57.4	
Median Ve	0.670	1.0	0.033	86.7	45.9	

*The AUC values were compared with 0.5 (random guess), †*p* value for the comparison of ROC curves was calculated with the methods by DeLong and Hanley & McNeil. AUC = area under the ROC curve, PV = percentile value, ROC = receiver operating characteristic

parameters that significantly differed in the two groups (mean Ktrans and median Ve). The AUC values of the mean Ktrans and median Ve were statistically significant for the prediction of EP (AUC = 0.684; $p = 0.021$, and AUC = 0.670; $p = 0.033$, respectively). There were no statistically significant differences among the AUCs of the three parameters (i.e., 95th PV Ktrans, mean Ktrans, and median Ve) after comparing the ROC curves using the DeLong's test and the Hanley & McNeil test ($p > 0.05$).

Table 3 and Figure 3 illustrate the diagnostic accuracy for distinguishing the EP and NEP groups using the optimal cutoff values for the three significant parameters (95th PV of the Ktrans, mean Ktrans, and median Ve).

The Ktrans, Ve, and nCBV maps for representative subjects of the EP and NEP groups are illustrated in Figures 4 and 5, respectively.

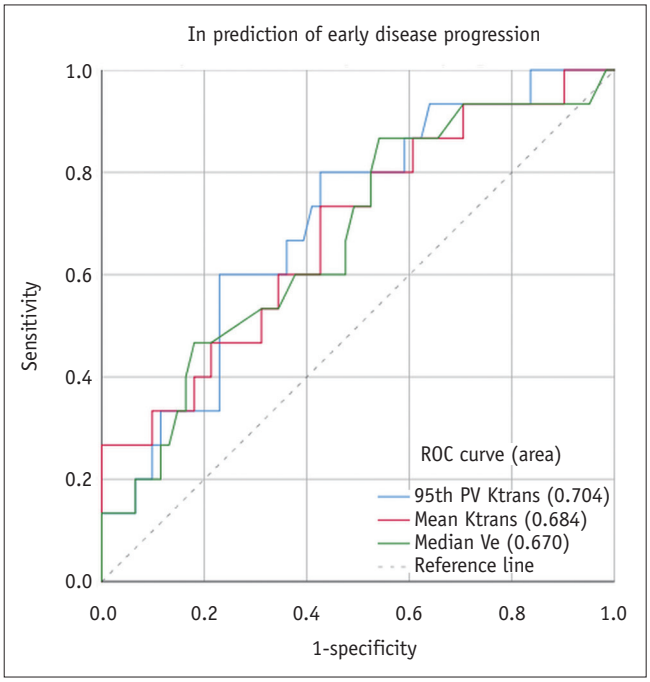

Fig. 3. ROC curves for the 95th PV of Ktrans ($p = 0.005$, AUC = 0.704), mean Ktrans ($p = 0.021$, AUC = 0.684), and median Ve ($p = 0.033$, AUC = 0.670). The AUC values were determined for the 6-month predicting early progression. The AUCs of the three parameters of dynamic contrast-enhanced MRI were significantly different from 0.5 (random guess) ($p < 0.05$). AUC = area under the ROC curve, PV = percentile value, ROC = receiver operating characteristic

Univariable Survival Analysis

The three statistically significant parameter values (95th PV of Ktrans, mean Ktrans, and median Ve) of DCE MRI were analyzed as prognostic markers of EP using univariable Cox proportional hazards regression. For predicting EP, the hazard ratio (HR) for the mean Ktrans was the highest among the DCE MRI parameters, followed by the 95th PV of Ktrans. However, the median Ve was not statistically significant for the prediction of EP in the univariable Cox regression analysis. The HRs for the univariable Cox regression of the three parametric values for predicting EP are presented in Table 4.

Multivariable Cox Proportional Hazard Regression

We included age, sex, 95th PV of Ktrans, and the mean Ktrans in the multivariable Cox proportional hazard regression analysis for EP prediction. Among these variables, only the 95th PV Ktrans was a significant independent predictor of EP (HR = 1.06; 95% confidence interval [CI] 1.02–1.11; $p < 0.009$); none of the clinical parameters or the mean Ktrans reached statistical significance.

Kaplan-Meier Survival Analysis

Kaplan-Meier survival analysis of the populations dichotomized according to the median value of the 95th PV of Ktrans (0.0312 min^{-1}) was performed, which revealed that this parameter remained a significant predictor of EP ($p = 0.045$). The high 95th PV of Ktrans group showed significantly shorter PFS than the low 95th PV of Ktrans patient group (the median PFS of the high and low 95th PV of Ktrans groups were 281 days [95% CI, 223.5–338.5 days] and 347 days [95% CI, 276.2–417.8 days], respectively). The Kaplan-Meier survival curves of the 95th PV of Ktrans are illustrated in Figure 6.

https://doi.org/10.3348/kjr.2020.1272

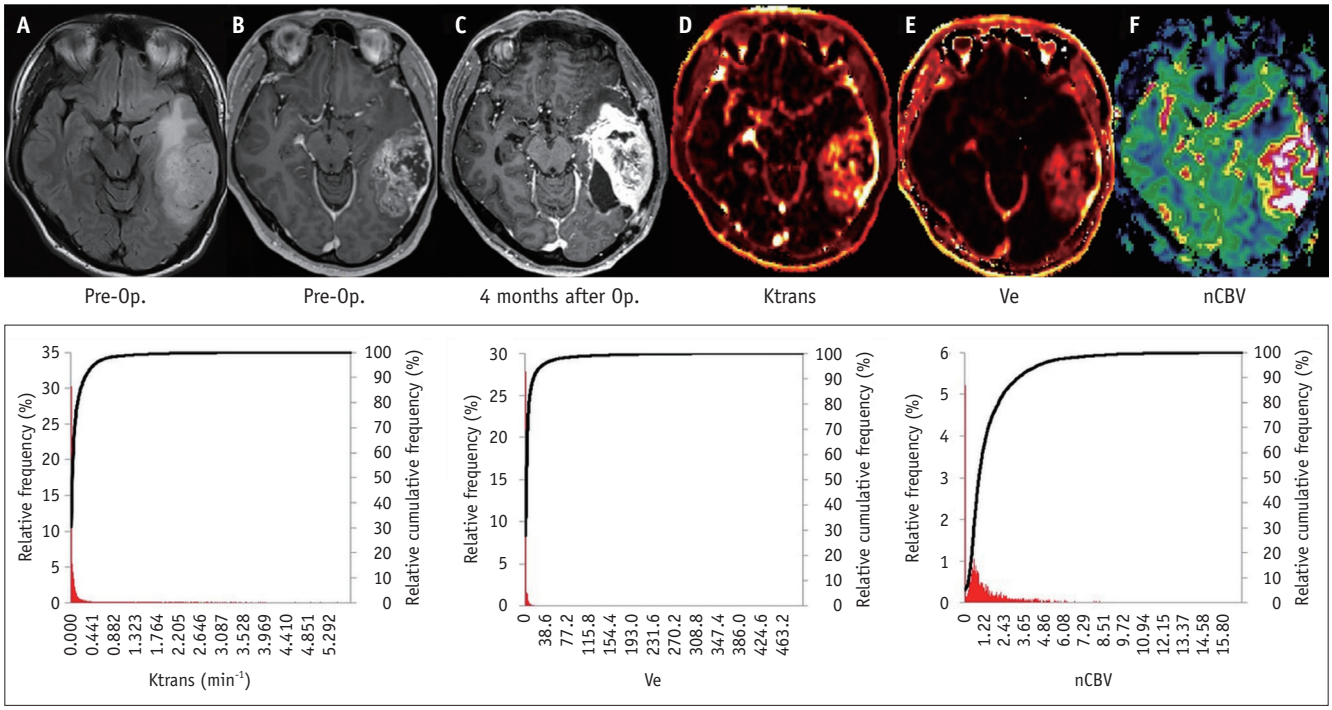

Fig. 4. Early disease progression (predicting EP = 4 months) in a 58-year-old male with GBM.
A-F. An irregularly enhancing mass with internal necrosis and non-enhancing, T2 HSI lesions at the left temporal lobe is illustrated on baseline structural FLAIR **(A)** and CE T1WI **(B)** as well as the perfusion and permeability parametric maps of Ktrans **(D)**, Ve **(E)** and nCBV **(F)**. After total surgical removal of the contrast-enhancing area of the GBM (not shown) and the completion of concomitant chemoradiotherapy with adjuvant temozolomide, a heterogeneously enhancing mass is shown on follow-up CE T1WI **(C)** (4 months after surgery) along the surgical margin, which is confirmed as early disease progression. The red bars and black lines in the cumulative histogram of the perfusion and permeability parameters (bottom row of the figure) show the distribution of Ktrans, Ve, and nCBV in the non-enhancing, peritumoral T2-HSI lesions. The cumulative histograms of Ktrans and Ve reveal less steep inclinations and wider transition areas than the corresponding cumulative histograms in figure 5, which indicates that the EP group has higher parametric values than the non-EP group. In this patient, the 95th PV of Ktrans and mean Ktrans values were 0.46 min^{-1} and 0.11 min^{-1}, respectively, which are higher than those of the patient in figure 5. CE = contrast-enhanced, EP = early progression, FLAIR = fluid-attenuated inverse recovery, GBM = glioblastoma, HSI = high-signal-intensity, nCBV = normalized relative cerebral blood volume, Op. = near total resection of contrast-enhancing portion, T1WI = T1-weighted image

DISCUSSION

This study revealed that higher parametric values of Ktrans and Ve from non-enhancing, T2-HSI lesions were correlated with EP in GBM patients who underwent total removal of the contrast-enhancing portion and CCRT. Multivariable Cox proportional hazard analysis revealed that the 95th PV of Ktrans was the only independent prognostic factor for PFS.

The non-enhancing, T2-HSI lesions of GBM are composed of peritumoral edema components and unenhanced microscopic infiltrative glioblastoma cells, which cause difficulties in predicting responses for patients with GBM. Several previous studies have investigated non-enhancing, T2-HSI lesions of GBM and their prognostic value [15-18]; however, these studies were based on nonquantitative image parameters and nonobjective criteria and also used only parts of slices from the MR images in their analyses. It may be difficult to represent the perfusion and permeability of an entire non-enhancing, T2-HSI lesion using this type of information.

Kim et al. [10] and Hwang et al. [19] recently reported that the preoperative Ktrans value had prognostic value in predicting the disease progression of GBM. Kim et al. [10] quantitatively analyzed non-enhancing, T2-HSI lesions of GBM using DCE MRI and showed that a higher PV of Ktrans (99th PV of Ktrans) was superior to the PVs of Ve and Vp in predicting the 1-year PFS of GBM patients. Hwang et al. [19] also quantitatively analyzed the whole volume of non-enhancing, T2-HSI lesions of GBM and revealed that PFS significantly correlated with the median Ktrans value of non-enhancing, T2-HSI lesions from preoperative DCE MRI. Our findings are consistent with the results of these recent studies and showed that the preoperative Ktrans of T2-HSI lesions may be a candidate imaging biomarker for EP.

Several studies have investigated the DSC MRI-derived

https://doi.org/10.3348/kjr.2020.1272

Korean Journal of Radiology
KJR

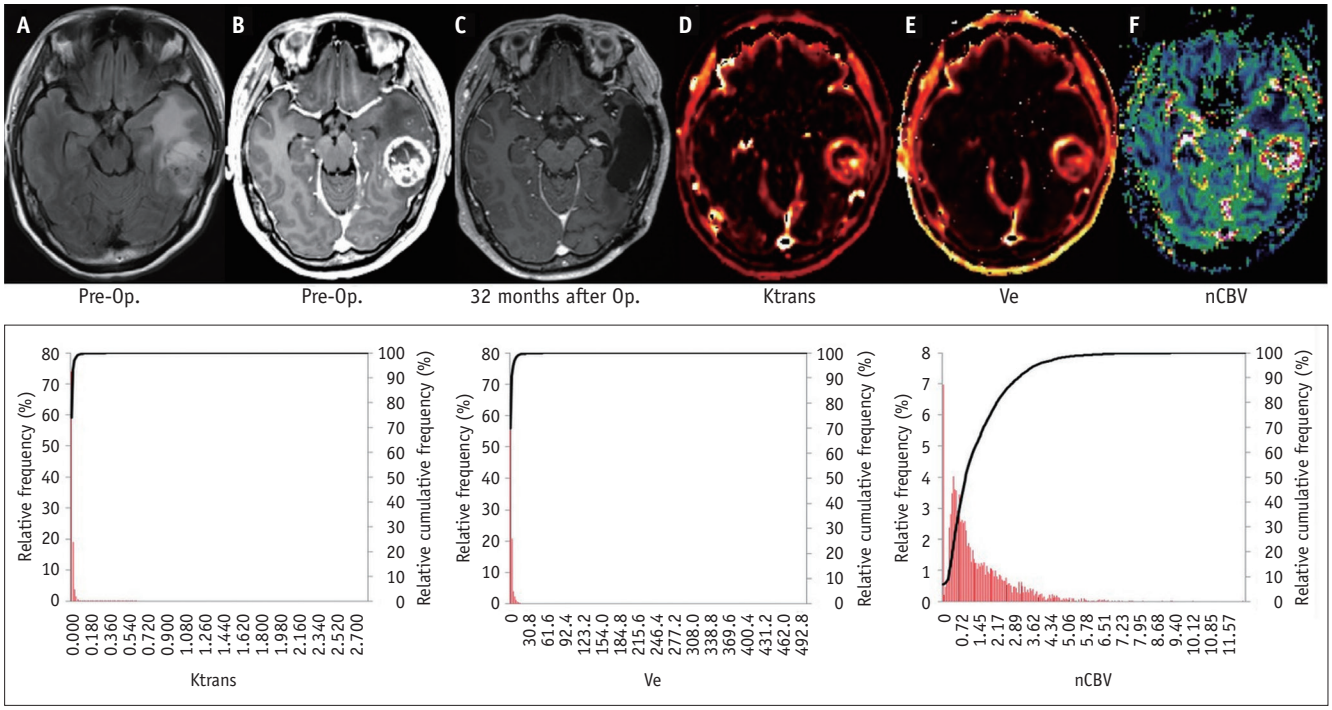

Fig. 5. Lack of progression (predicting EP = 37 months) in a 56-year-old female with GBM.
A-F. An enhancing mass with internal necrosis and non-enhancing, T2 HSI lesions at the left temporal lobe is demonstrated on baseline structural FLAIR **(A)** and contrast-enhanced T1WI **(B)** as well as the perfusion and permeability parametric maps of Ktrans **(D)**, Ve **(E)** and nCBV **(F)**. After total surgical removal of the contrast-enhancing area of the GBM (not shown) and the completion of concomitant chemoradiotherapy with adjuvant temozolomide, this patient was diagnosed with nonprogression on a follow-up MRI **(C)** performed 32 months after surgery. The cumulative histograms of the perfusion and permeability parameters (Ktrans, Ve, and nCBV) are shown at the bottom row of the figure. The red bars and black lines indicate the relative frequencies of the perfusion and permeability parameters in the non-enhancing, T2-HSI lesions. The cumulative histograms of Ktrans and Ve show a left shift relative to those in figure 4, which means that the non-EP group has lower parametric values than the EP group. In this patient, the 95th PV of Ktrans and the mean Ktrans values were 0.02 min^{-1} and 0.005 min^{-1}, respectively, which were lower than those of the patient in figure 4. EP = early progression, FLAIR = fluid-attenuated inverse recovery, GBM = glioblastoma, HSI = high-signal-intensity, nCBV = normalized relative cerebral blood volume, Op. = near total resection of contrast-enhancing portion, T1WI = T1-weighted image

parameters (e.g., the CBV) of non-enhancing, T2-HSI lesions to determine their prognostic value for GBM patients, but some discrepancies are present among these studies. Jain et al. [9] defined the mean CBV of three regions of interest (ROIs) for non-enhancing, T2-HSI lesions (on FLAIR images) within 1 cm of the contrast-enhancing portion of the GBM as the relative CBV (rCBV) of the lesions. They reported that the rCBV showed a significant prognostic prediction of 1-year overall survival (OS) and PFS, which was longer than that of the present study. Although the rCBV of the non-enhancing, T2-HSI lesions was assessed quantitatively, the rCBV information from the entire volume of the non-enhancing, T2-HSI lesions was not measured. Juan-Albarracín et al. [20] used the hemodynamic tissue signature method to analyze the vascular characteristics of the contrast-enhancing portion and non-enhancing, T2-HSI lesions of GBM. They reported that the rCBVmax of the infiltrative peripheral edema in the non-enhancing, T2-HSI lesions revealed a significant correlation with patient survival. However, the rCBVmax of the vasogenic peripheral edema was not significantly correlated with survival in the Cox regression analysis. The Kaplan-Meier survival analysis showed no significant survival difference between the groups delimited by higher and lower rCBVmax values for infiltrative peripheral edema and vasogenic peripheral edema of non-enhancing, T2-HSI lesions. Akbari et al. [21] trained a support vector machine using ROIs to create heterogeneity maps and found that the rCBV of non-enhancing, T2-HSI lesions did not correlate with survival. Our findings concur with those of some studies, as our preoperative CBV of T2-HSI lesions of GBM was not significantly correlated with EP.

Non-enhancing peritumoral T2-HSI lesions of GBM are better referred to as infiltrative edema because they represent vasogenic edema and infiltrating tumor cells that penetrate the blood-brain barrier and generally invade

https://doi.org/10.3348/kjr.2020.1272

Table 4. Univariable Cox Regression Analysis of Dynamic Contrast-Enhanced MR Imaging-Derived Permeability Parameters*

Parameter	Hazard Ratio (95% CI)*	*P*
95th PV Ktrans	1.06 (1.02–1.11)	0.009
Mean Ktrans	1.25 (1.04–1.51)	0.017
Median Ve	1.04 (0.93–1.16)	0.458

*Hazard ratios for Ktrans were adjusted to a unit change of 0.01 min^{-1}. CI = confidence of interval, PV = percentile value

the white matter tracts [22]. In conditions associated with increased capillary permeability caused by GBM, the extravasation of plasma fluid and proteins occurs, which leads to vasogenic edema and increased interstitial fluid pressure [23]. This subsequently increases intracranial pressure and reduces cerebral perfusion pressure and cerebral blood flow, which could lead to brain ischemia [24]. The uptake of contrast by tumor tissue is likely flow-limited rather than permeability-limited because of the abnormal vasculature of GBM tumors, and the non-enhancing, infiltrative tumor portion of the non-enhancing, T2-HSI lesions may indicate a significantly reduced blood flow than that of the contrast-enhancing portion [22]. Therefore, when predicting prognosis using non-enhancing, T2-HSI lesions of GBM, the permeability parameters of DCE may be more appropriate imaging biomarkers than those of DSC.

In this study, even though the 95th PV of Ktrans had an independent predictive value for EP, HR was not very high (1.062) on Cox regression analysis. For the non-enhancing, T2-HSI lesions, the blood-brain barrier is less disrupted compared with that of the contrast-enhancing area of GBM. Moreover, the difference in permeability caused by microscopic infiltrating tumor cells is lower than that of contrast-enhancing lesions [25]. As a result, it may be difficult to detect a slight difference in permeability caused by tumor cells; it is possible that the corresponding risk was measured to a lesser extent. The other possible reason is that when permeability increases, the delivery of temozolomide into brain tissues and the effect of chemotherapy increases [26,27]. Therefore, we speculate that the risk of increasing Ktrans was reduced due to the increased chemotherapy effect.

In contrast with previous studies, we used a 6-month progression-free survival (6-month PFS) as the prognostic prediction endpoint. For the prognostic prediction of GBM patients, the 12-month OS has been regarded as the most objective indicator because it is easy to identify and simple to interpret. However, the 12-month OS has several major

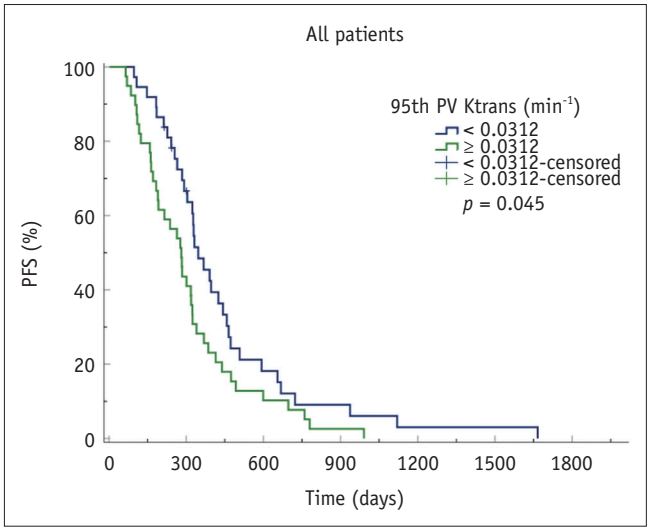

Fig. 6. Kaplan-Meier curves according to the 95th PV of Ktrans for non-enhancing, T2-HSI lesions. The high 95th PV of Ktrans group showed a significantly shorter PFS than the low 95th PV of Ktrans patient group (p = 0.045). The median PFS of the high and low 95th PV of Ktrans patient groups was 281 days (95% CI, 223.5–338.5 days) and 347 days (95% CI, 276.2–417.8 days), respectively (p = 0.045). CI = confidence interval, HSI = high-signal-intensity, PFS = progression-free survival, PV = percentile value

limitations. First, it can be affected by subsequent life-prolonging treatment after the patients exit the research. Investigators must also wait for a longer duration than the 6-month PFS before the research results are known. There is increasing evidence that the 6-month PFS can serve as an appropriate alternative primary endpoint for OS in newly diagnosed GBM because of its high correlation with the 12-month OS [28-30]. For this reason, the two generally used endpoints of phase II clinical trials for newly diagnosed GBM in recent years are 6-month PFS and 12-month OS [29].

In addition to the intrinsic limitations of any retrospective study, several other limitations of our study should be considered. First, because of the manual determination of the volume of interest (VOI), there may be issues related to subjectivity and low reproducibility. However, using the aforementioned subtraction of the two VOI masks, we defined the margins of the true non-enhancing, T2-HSI lesions with confidence. Second, in this study, we gathered patients who were administered a double dose of gadolinium-based contrast agent (GBCA) for the DSC MRI and DCE MRI scans. These exposures may increase the chance of nephrogenic systemic fibrosis and gadolinium organ tissue deposition [31,32]. Although macrocyclic GBCA was administered for this study, the risk of gadolinium deposition may be increased in patients

https://doi.org/10.3348/kjr.2020.1272

Korean Journal of Radiology
KJR

who receive a double dose of GBCA. A previous study proposed the administration of 1 dose of GBCA for both DSC and DCE MR imaging by dividing the dose, which could preclude double injections in the future [33]. Third, the small sample size of the EP group (15 patients) may not provide sufficient power to reveal a statistically significant difference between the diagnostic accuracies of DSC and DCE MRI parameters for the prediction of PFS for GBM patients.

In conclusion, the DCE MRI permeability parameters from non-enhancing, T2-HSI lesions in GBM patients were better candidates for prognostic imaging biomarkers than DSC MRI perfusion parameters. The 95th PV of Ktrans was the most important parameter for the prediction of EP of GBM. It may be helpful to apply the 95th PV of Ktrans to the risk-stratified treatment of GBM patients.

Supplement

The Supplement is available with this article at https://doi.org/10.3348/kjr.2020.1272.

Conflicts of Interest

The authors have no potential conflicts of interest to disclose.

Author Contributions

Conceptualization: Seung Hong Choi. Data curation: Sang Won Jo, Eun Jung Lee. Formal analysis: Sang Won Jo. Funding acquisition: Seung Hong Choi. Investigation: Sang Won Jo, Tae Jin Yun, Ji-Hoon Kim. Methodology: Sang Won Jo, Roh-Eul Yoo, Koung Mi Kang. Software: Sang Won Jo, Roh-Eul Yoo, Koung Mi Kang. Supervision: Chul-Ho Sohn. Writing—original draft: Sang Won Jo. Writing—review & editing: Seung Hong Choi.

ORCID iDs

Sang Won Jo
https://orcid.org/0000-0002-9542-7378
Seung Hong Choi
https://orcid.org/0000-0002-0412-2270
Eun Jung Lee
https://orcid.org/0000-0002-2933-2995
Roh-Eul Yoo
https://orcid.org/0000-0002-5625-5921
Koung Mi Kang
https://orcid.org/0000-0001-9643-2008
Tae Jin Yun
https://orcid.org/0000-0001-8441-4574
Ji-Hoon Kim
https://orcid.org/0000-0002-6349-6950
Chul-Ho Sohn
https://orcid.org/0000-0003-0039-5746

REFERENCES

1. Stupp R, Mason WP, van den Bent MJ, Weller M, Fisher B, Taphoorn MJ, et al. Radiotherapy plus concomitant and adjuvant temozolomide for glioblastoma. *N Engl J Med* 2005;352:987-996
2. Stummer W, Pichlmeier U, Meinel T, Wiestler OD, Zanella F, Reulen HJ; ALA-Glioma Study Group. Fluorescence-guided surgery with 5-aminolevulinic acid for resection of malignant glioma: a randomised controlled multicentre phase III trial. *Lancet Oncol* 2006;7:392-401
3. Idoate MA, Díez Valle R, Echeveste J, Tejada S. Pathological characterization of the glioblastoma border as shown during surgery using 5-aminolevulinic acid-induced fluorescence. *Neuropathology* 2011;31:575-582
4. Chamberlain MC. Radiographic patterns of relapse in glioblastoma. *J Neurooncol* 2011;101:319-323
5. Dobelbower MC, Burnett Iii OL, Nordal RA, Nabors LB, Markert JM, Hyatt MD, et al. Patterns of failure for glioblastoma multiforme following concurrent radiation and temozolomide. *J Med Imaging Radiat Oncol* 2011;55:77-81
6. McDonald MW, Shu HK, Curran WJ Jr, Crocker IR. Pattern of failure after limited margin radiotherapy and temozolomide for glioblastoma. *Int J Radiat Oncol Biol Phys* 2011;79:130-136
7. Burger PC, Heinz ER, Shibata T, Kleihues P. Topographic anatomy and CT correlations in the untreated glioblastoma multiforme. *J Neurosurg* 1988;68:698-704
8. Parsa AT, Wachhorst S, Lamborn KR, Prados MD, McDermott MW, Berger MS, et al. Prognostic significance of intracranial dissemination of glioblastoma multiforme in adults. *J Neurosurg* 2005;102:622-628
9. Jain R, Poisson LM, Gutman D, Scarpace L, Hwang SN, Holder CA, et al. Outcome prediction in patients with glioblastoma by using imaging, clinical, and genomic biomarkers: focus on the nonenhancing component of the tumor. *Radiology* 2014;272:484-493
10. Kim R, Choi SH, Yun TJ, Lee ST, Park CK, Kim TM, et al. Prognosis prediction of non-enhancing T2 high signal intensity lesions in glioblastoma patients after standard treatment: application of dynamic contrast-enhanced MR imaging. *Eur Radiol* 2017;27:1176-1185
11. Kim SH, Cho KH, Choi SH, Kim TM, Park CK, Park SH, et al. Prognostic predictions for patients with glioblastoma after standard treatment: application of contrast leakage information from DSC-MRI within nonenhancing FLAIR high-

signal-intensity lesions. *AJNR Am J Neuroradiol* 2019;40:2052-2058
12. Wen PY, Macdonald DR, Reardon DA, Cloughesy TF, Sorensen AG, Galanis E, et al. Updated response assessment criteria for high-grade gliomas: response assessment in neuro-oncology working group. *J Clin Oncol* 2010;28:1963-1972
13. Jung SC, Choi SH, Yeom JA, Kim JH, Ryoo I, Kim SC, et al. Cerebral blood volume analysis in glioblastomas using dynamic susceptibility contrast-enhanced perfusion MRI: a comparison of manual and semiautomatic segmentation methods. *PLoS One* 2013;8:e69323
14. Tozer DJ, Jäger HR, Danchaivijitr N, Benton CE, Tofts PS, Rees JH, et al. Apparent diffusion coefficient histograms may predict low-grade glioma subtype. *NMR Biomed* 2007;20:49-57
15. Hammoud MA, Sawaya R, Shi W, Thall PF, Leeds NE. Prognostic significance of preoperative MRI scans in glioblastoma multiforme. *J Neurooncol* 1996;27:65-73
16. Pope WB, Sayre J, Perlina A, Villablanca JP, Mischel PS, Cloughesy TF. MR imaging correlates of survival in patients with high-grade gliomas. *AJNR Am J Neuroradiol* 2005;26:2466-2474
17. Schoenegger K, Oberndorfer S, Wuschitz B, Struhal W, Hainfellner J, Prayer D, et al. Peritumoral edema on MRI at initial diagnosis: an independent prognostic factor for glioblastoma? *Eur J Neurol* 2009;16:874-878
18. Wu CX, Lin GS, Lin ZX, Zhang JD, Liu SY, Zhou CF. Peritumoral edema shown by MRI predicts poor clinical outcome in glioblastoma. *World J Surg Oncol* 2015;13:97
19. Hwang I, Choi SH, Park CK, Kim TM, Park SH, Won JK, et al. Dynamic contrast-enhanced MR imaging of nonenhancing T2 high-signal-intensity lesions in baseline and posttreatment glioblastoma: temporal change and prognostic value. *AJNR Am J Neuroradiol* 2020;41:49-56
20. Juan-Albarracín J, Fuster-Garcia E, Pérez-Girbés A, Aparici-Robles F, Alberich-Bayarri Á, Revert-Ventura A, et al. Glioblastoma: vascular habitats detected at preoperative dynamic susceptibility-weighted contrast-enhanced perfusion MR imaging predict survival. *Radiology* 2018;287:944-954
21. Akbari H, Macyszyn L, Da X, Wolf RL, Bilello M, Verma R, et al. Pattern analysis of dynamic susceptibility contrast-enhanced MR imaging demonstrates peritumoral tissue heterogeneity. *Radiology* 2014;273:502-510
22. Cha S. Update on brain tumor imaging: from anatomy to physiology. *AJNR Am J Neuroradiol* 2006;27:475-487
23. Bruce JN, Criscuolo GR, Merrill MJ, Moquin RR, Blacklock JB, Oldfield EH. Vascular permeability induced by protein product of malignant brain tumors: inhibition by dexamethasone. *J Neurosurg* 1987;67:880-884
24. Esquenazi Y, Lo VP, Lee K. Critical care management of cerebral edema in brain tumors. *J Intensive Care Med* 2017;32:15-24
25. Kang Y, Hong EK, Rhim JH, Yoo RE, Kang KM, Yun TJ, et al. Prognostic value of dynamic contrast-enhanced MRI-derived pharmacokinetic variables in glioblastoma patients: analysis of contrast-enhancing lesions and non-enhancing T2 high-signal intensity lesions. *Korean J Radiol* 2020;21:707-716
26. Gerstner ER, Emblem KE, Chang K, Vakulenko-Lagun B, Yen YF, Beers AL, et al. Bevacizumab reduces permeability and concurrent temozolomide delivery in a subset of patients with recurrent glioblastoma. *Clin Cancer Res* 2020;26:206-212
27. Yoo RE, Choi SH, Kim TM, Park CK, Park SH, Won JK, et al. Dynamic contrast-enhanced MR imaging in predicting progression of enhancing lesions persisting after standard treatment in glioblastoma patients: a prospective study. *Eur Radiol* 2017;27:3156-3166
28. Polley MY, Lamborn KR, Chang SM, Butowski N, Clarke JL, Prados M. Six-month progression-free survival as an alternative primary efficacy endpoint to overall survival in newly diagnosed glioblastoma patients receiving temozolomide. *Neuro Oncol* 2010;12:274-282
29. Ballman KV, Buckner JC, Brown PD, Giannini C, Flynn PJ, LaPlant BR, et al. The relationship between six-month progression-free survival and 12-month overall survival end points for phase II trials in patients with glioblastoma multiforme. *Neuro Oncol* 2007;9:29-38
30. Han K, Ren M, Wick W, Abrey L, Das A, Jin J, et al. Progression-free survival as a surrogate endpoint for overall survival in glioblastoma: a literature-based meta-analysis from 91 trials. *Neuro Oncol* 2014;16:696-706
31. Yang L, Krefting I, Gorovets A, Marzella L, Kaiser J, Boucher R, et al. Nephrogenic systemic fibrosis and class labeling of gadolinium-based contrast agents by the Food and Drug Administration. *Radiology* 2012;265:248-253
32. McDonald RJ, McDonald JS, Dai D, Schroeder D, Jentoft ME, Murray DL, et al. Comparison of gadolinium concentrations within multiple rat organs after intravenous administration of linear versus macrocyclic gadolinium chelates. *Radiology* 2017;285:536-545
33. McGehee BE, Pollock JM, Maldjian JA. Brain perfusion imaging: how does it work and what should I use? *J Magn Reson Imaging* 2012;36:1257-1272

https://doi.org/10.3348/kjr.2020.1272